# High-Frequency Ultrasonic Imaging of the Anterior Segment Using an Annular Array Transducer

*Ronald H. Silverman, PhD,*[1,2] *Jeffrey A. Ketterling, PhD,*[1] *D. Jackson Coleman, MD*[1]

***Objective:*** Very high-frequency ultrasound (VHFU; >35 megahertz [MHz]) allows imaging of anterior segment structures of the eye with a resolution of less than 40 $\mu$m. The low focal ratio of VHFU transducers, however, results in a depth of field (DOF) of less than 1 mm. The aim was to develop a high-frequency annular array transducer for ocular imaging with improved DOF, sensitivity, and resolution compared with conventional transducers.

***Design:*** Experimental study.

***Participants:*** Cadaver eyes, ex vivo cow eyes, in vivo rabbit eyes.

***Methods:*** A spherically curved annular array ultrasound transducer was fabricated. The array consisted of 5 concentric rings of equal area, had an overall aperture of 6 mm, and a geometric focus of 12 mm. The nominal center frequency of all array elements was 40 MHz. An experimental system was designed in which a single array element was pulsed and echo data were recorded from all elements. By sequentially pulsing each element, echo data were acquired for all 25 transmit-and-receive annuli combinations. The echo data then were focused synthetically and composite images were produced. Transducer operation was tested by scanning a test object consisting of a series of 25-$\mu$m diameter wires spaced at increasing range from the transducer. Imaging capabilities of the annular array were demonstrated in ex vivo bovine, in vivo rabbit, and human cadaver eyes.

***Main Outcome Measures:*** Depth of field, resolution, and sensitivity.

***Results:*** The wire scans verified the operation of the array and demonstrated a 6.0-mm DOF, compared with the 1.0-mm DOF of a conventional single-element transducer of comparable frequency, aperture, and focal length. B-mode images of ex vivo bovine, in vivo rabbit, and cadaver eyes showed that although the single-element transducer had high sensitivity and resolution within 1 to 2 mm of its focus, the array with synthetic focusing maintained this quality over a 6-mm DOF.

***Conclusions:*** An annular array for high-resolution ocular imaging has been demonstrated. This technology offers improved DOF, sensitivity, and lateral resolution compared with single-element fixed focus transducers currently used for VHFU imaging of the eye. *Ophthalmology 2007;114:816–822 © 2007 by the American Academy of Ophthalmology.*

Ultrasonic imaging allows noninvasive visualization of ocular anatomic and pathologic features, even in the presence of optical opacities. Factors that impact on the overall usefulness of ultrasound systems include resolution, penetration, speed (frames/second), sensitivity (signal/noise), and depth of field (DOF). Resolution generally improves (and penetration declines) with frequency. Very high-frequency ultrasound (>35 megahertz [MHz]) provides an axial resolution of <40 $\mu$m, allowing exquisitely detailed depiction of anatomic structures. However, attenuation at this frequency is high, even in water, limiting clinical imaging in this frequency range to the anterior segment.

Clinical very high-frequency ultrasound, or ultrasound biomicroscopy, systems were introduced more than a decade ago[1–3] and have been used for imaging and biometric characterization of the cornea,[4–7] glaucoma diagnosis,[8,9] visualization of lens implants,[10,11] and diagnosis of tumors,[12] cysts,[13] and foreign bodies.[14] These systems use mechanically scanned, single-element, spherically focused transducers. The function of the transducer is to convert an electrical pulse into an acoustic pulse and then to convert echoes from tissue structures back into voltages from which images are formed. As the ratio, $F$ (focal length/aperture), of the transducer decreases, lateral resolution in the focal plane improves, but DOF degrades. For a 50-MHz transducer with an aperture, $a$, of 6 mm and focal length, $L$, of 12 mm, the

Originally received: March 7, 2006.
Accepted: July 7, 2006. Manuscript no. 2006-292.

[1] Department of Ophthalmology, Weill Medical College of Cornell University, New York, New York.

[2] Frederic L. Lizzi Center for Biomedical Engineering, Riverside Research Institute, New York, New York.

Supported by the National Institutes of Health, Bethesda, Maryland (grant nos. EB00238, EY014371), and Research to Prevent Blindness, Inc., New York, New York.

The authors have no proprietary interests related to the article.

Correspondence to Ronald H. Silverman, PhD, Department of Ophthalmology, Weill Medical College of Cornell University, 1300 York Avenue, Room K808, New York, NY 10021. E-mail: ros2012@med.cornell.edu.



ISSN 0161-6420/07/$–see front matter
doi:10.1016/j.ophtha.2006.07.050

expected DOF is 0.85 mm (from DOF = $7.08\lambda F^2$, where $\lambda$ = wavelength and $F = L/a$).[15] Outside this small region, signal amplitude and resolution fall precipitously. Experienced users of ultrasound biomicroscopy systems are quite familiar with this sweet spot, which constrains what can be seen in any one image.

Linear array transducers are composed of numerous independent transducer elements. A linear array can be synthetically focused electronically, unlike single-element transducers, which are constrained to focus at a fixed point. Linear arrays, however, are not currently commercially available at frequencies of more than 15 MHz because of difficulties in fabrication[16] (individual transducer elements are a wavelength in dimension) and the unavailability of control electronics.[17] Annular arrays, in which independent transducer elements are arranged in concentric rings, can be focused synthetically without the constraint of small element sizes and complicated electronics. Focusing is accomplished by applying appropriate time delays to the excitation pulses and the echoes received by each element (Fig 1). Although an annular array cannot be electronically steered laterally, as can a linear array, it can be as compact as a fixed-focus single-element transducer and thus can fit in a typical hand-held sector scan probe housing.

Annular arrays can be fabricated with no curvature (i.e., flat),[18,19] with a spherical lens[20] or with a spherical geometry.[21,22] Although the principle of dynamic focusing is the same for all, spherically curved devices are advantageous compared with flat arrays because fewer elements are required to achieve the same improvement in DOF. Spherical curvature also leads to better lateral resolution for 2 transducers of similar aperture and number of elements.

This report describes a prototype 40-MHz spherically curved annular array and testing of its performance in imaging of the anterior segment of the eye.

## Materials and Methods

The spherically curved annular array developed for these studies consisted of 5 concentric rings of equal area. The piezoelectric material used to send and receive ultrasound pulses was a 9-$\mu$m thick polyvinylidene fluoride membrane (Ktech Corp., Albuquerque, NM) providing a nominal center frequency of 40 MHz. This was bonded to a copper-clad polyamide film (RFlex 1000L810; Rogers Corp., Chandler, AZ) on which the array pattern was formed using standard printed circuit board techniques. The 6-mm diameter array then was pressed against a steel sphere to produce a 12-mm radius of curvature. The array was fitted into a UHF connector to provide mechanical protection and electrical shielding (Fig 2). Fabrication is described in greater detail by Ketterling et al.[21]

We developed a LabVIEW program (National Instruments, Austin, TX) to control the components of the PC-based scanning system, including the pulser, the switching unit, receiver channels, and the 3 orthogonal linear motion stages used for scanning. During scanning, the transducer is mechanically translated and pulses are emitted at evenly spaced positions. In a conventional system using a single-element transducer, 1 pulse/echo data record is acquired at each position. With an n-element annular array, however, it is necessary to acquire $n^2$ records per position: 1 for each possible send-and-receive pair. Hence, 25 pulse/echo records must be acquired per position with the 5-element array. To accomplish this, 5 scans were performed to form a single image: 1 scan for each pulsed ring, with echo data recorded from all 5 rings (Fig 3). Simple addition of all 25 echo sequences produces an echo sequence equivalent to that of a focused single-element transducer. However, by adding appropriate time delays to the digitized echo

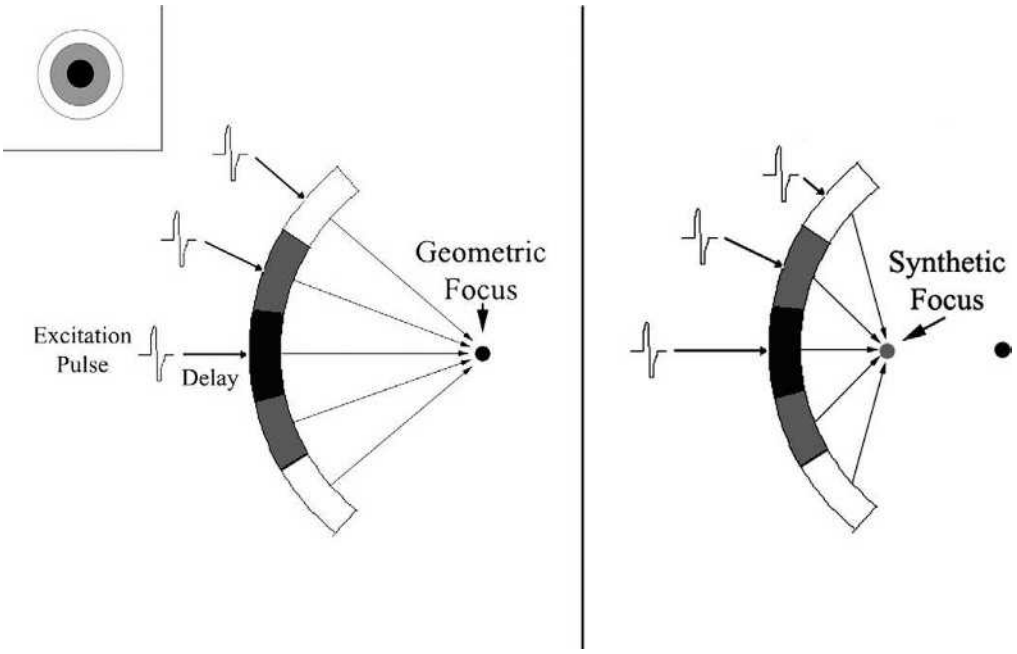


**Figure 1.** Schematic illustration of the operation of a curved annular array. The figure shows a 3-element array in cross section and en face (insert). **Left**, When all the array elements are excited simultaneously, the wavefronts from each element will converge at the geometric focus. **Right**, Here, the outermost ring is excited first and the central ring last, resulting in convergence of wavefronts at a synthetic focal point closer than the geometric focus.

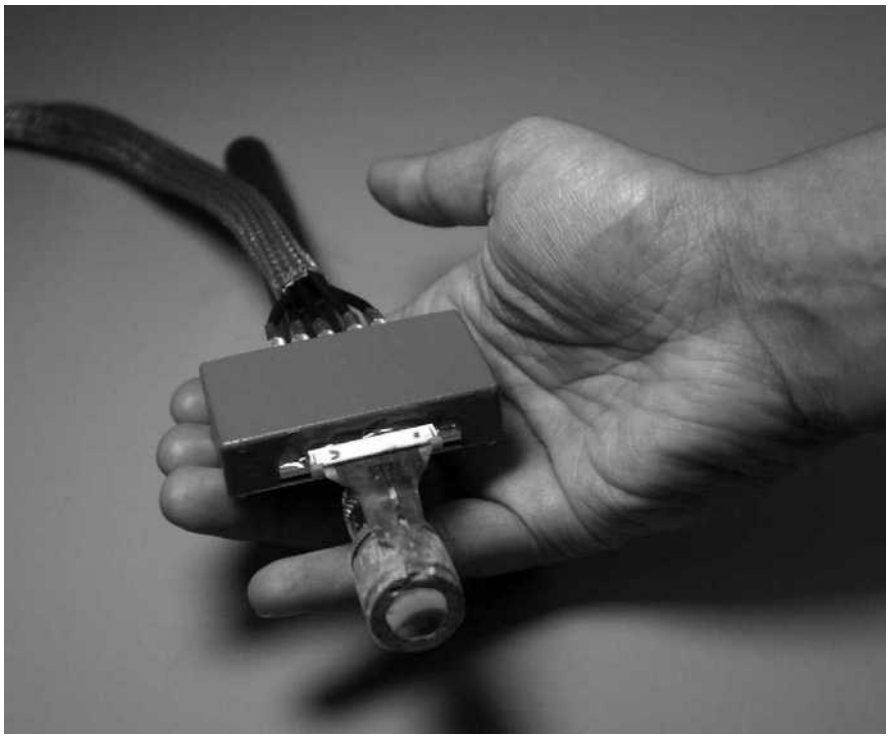

**Figure 2.** Photograph of a prototype annular array and flex circuit containing the electronic fan-out.

data from each send-and-receive ring pair and then summing, synthetic focusing can be achieved at any axial depth.[21] We produced composite, synthetically focused images by merging synthetically focused data over a series of 41 focal zones of increasing depth. Acquisition time for a single synthetically focused image was approximately 40 seconds.

The array was tested initially by scanning a series of 25-$\mu$m diameter wires arranged in 1-mm intervals of increasing depth. The performance of the array was compared with that of a single-element transducer of similar center frequency, bandwidth, aperture, and focal length (PI50-2 polyvinylidene fluoride-based 40-MHz transducer, Panametric-NDT, Waltham, MA; 6-mm aperture; 12-mm focal length).

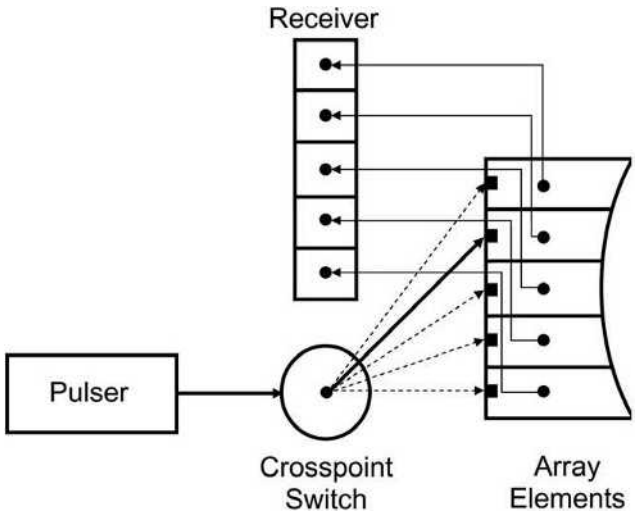


**Figure 3.** Diagram illustrating how, during scanning, the crosspoint switch directs excitation pulses to only 1 of the 5 transducer elements at a time (solid arrow), whereas echo data are collected from all 5 channels. To acquire all 25 possible send-and-receive pairs needed to form an image, the transducer is scanned 5 times, once for each excited element.

The ocular imaging capabilities of the annular array were evaluated in ex vivo bovine, in vivo rabbit, and human cadaver eyes. Institutional review board/ethics committee approval was obtained for the use of human tissues. Animal experimentation was performed in compliance with the Association for Research in Vision and Ophthalmology Resolution on the Use of Animals in Research and under a protocol approved by the Institutional Animal Care and Use Committee of the Weill Medical College of Cornell University.

We compared the performance of the array with that of the single-element transducer in imaging the anterior segment. The array was tested with simple addition of the individual channels (simulating a single-element transducer) and with synthetic focusing. Consecutive scans were made of each eye, decreasing the range between the transducer and the eye by 1-mm steps, allowing assessment of image quality as the geometric focus of the transducer was moved depthwise through the anterior segment.

## Results

Comparative images of 25-$\mu$m wires obtained with the single-element transducer and the annular array in both summed and synthetic focus modes are shown in Figure 4. Note the decreased sensitivity and lateral spreading of wire targets outside the 12-mm geometric focus in images made with the single-element probe or when the array is operated without synthetic focus.

Figures 5 and 6 are scans of ex vivo cow eyes. In Figure 5, the eye was scanned parallel to and through the optic axis, with echo complexes acquired from the cornea and anterior lens surface. The figure compares images produced with and without synthetic fo-

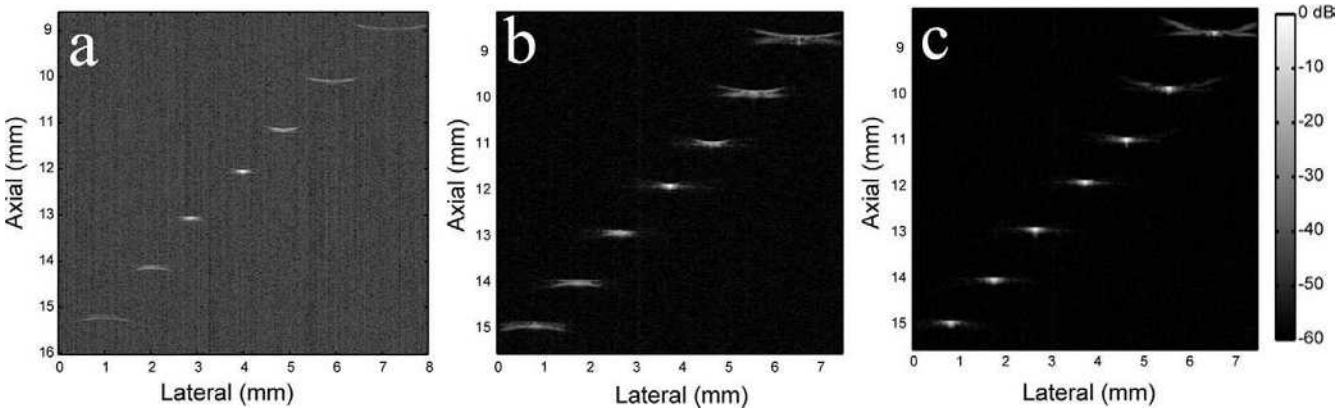


**Figure 4.** B-mode images of a series of wire targets at increasing ranges about the geometric focus with (**a**) a focused single-element transducer, (**b**) the array without synthetic focusing, and (**c**) the array with synthetic focus processing. Where synthetic focusing is not used, the array functions as the equivalent of a conventional single-element transducer. Note the improved lateral resolution obtained outside the geometric focus when synthetic focusing is used. Also note the improvement in dynamic range (reduced noise) in the array compared with the single-element transducer. dB = decibels.

cusing. Synthetic focusing allowed simultaneous high-resolution visualization of the cornea and lens, which are more than 3 mm apart (similar to a typical human anterior chamber depth). The results demonstrate the improved signal-to-noise ratio (SNR) achieved when the data are processed with the synthetic focusing algorithm. This SNR improvement resulted from the increase in echo amplitude as the time-shifted echo data from each array transmit-and-receive pair were summed coherently, whereas the random background noise underwent an averaging effect. The improvement in SNR became more pronounced when the strongest reflectors were situated away from the geometric focus. Figure 6 illustrates the improved DOF obtained using synthetic focusing. Here, a single-element transducer is compared with the annular array in summed and synthetic focus modes. Both the single-element (Fig 6a) and array data with no delay corrections (Fig 6b) revealed a zone of high sensitivity and high resolution limited to the cornea (where the geometric focus was situated), whereas the iris and lens echoes were seen at reduced amplitude and resolution. These 2 images are qualitatively identical because the summed data with no delay corrections simulated a single-element transducer with a 6-mm aperture and 12-mm focal length. After synthetic focusing was applied to the array data (Fig 6c), the iris and lens were brighter and sharper and the angle was seen more clearly, demonstrating improved DOF and lateral resolution.

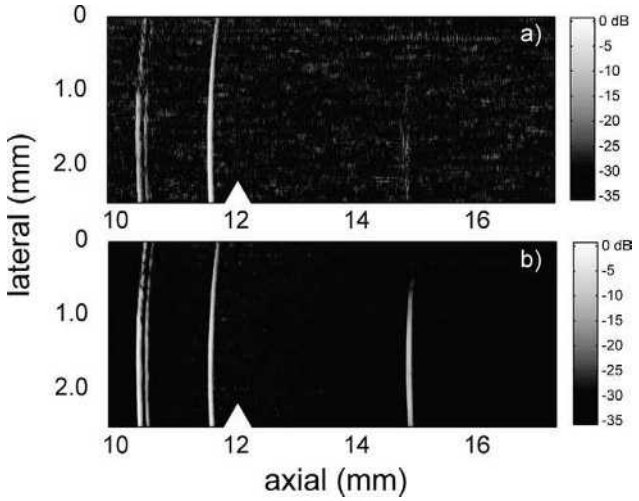


**Figure 5.** Central cornea and anterior lens surface of an ex vivo bovine eye scanned with the annular array with (**a**) no delay corrections and (**b**) synthetic focusing (41 focal zones, 180 $\mu$m/zone). The interfaces seen in the image include (from left to right) the epithelial surface, Bowman's membrane, posterior corneal surface, and anterior lens surface. The position of the geometric focus at 12 mm is indicated by white triangles. The signal-to-noise ratios were (**a**) 26 decibels (dB) and (**b**) 34 dB. Note the much improved depiction of the anterior cornea (near field) and lens surface (far field) with synthetic focus.

An in vivo anterior segment scan of a rabbit eye is shown in Figure 7. The summed data with no delay corrections (Fig 7a) revealed the cornea and lens, but the iris, angle, and ciliary body were visualized poorly. After synthetic focusing (Fig 7b), an improved delineation of the angle and ciliary processes was observed and the SNR was improved by 6 dB. Despite environmental electrical noise, the in vivo rabbit results emphasize how an annular array is able to resolve ocular features spanning more than 5 mm of axial range.

The anterior segment of a human cadaver eye was scanned (Figs 8, 9). Figure 8 shows an image formed from just the center element of the array ($F = 4.9$; Fig 8a), from the full array with no delay corrections ($F = 2$; Fig 8b), and with synthetic focusing (Fig 8c). The center element image demonstrated a larger DOF than the full array aperture, as would be expected because of the higher $F$ value, but at the sacrifice of resolution. The synthetically focused image (Fig 8c) again demonstrated improved image quality. Even though the geometric focus was located in front of the cornea, the deeper tissue features, such as the iris, were well defined. The effect of range on image quality is demonstrated in Figure 9. The 2 series of images show the appearance of the anterior segment of a cadaver eye as the range between the eye and the transducer was decreased by 1-mm increments. The top and bottom series consist of images generated without and with synthetic focus, respectively. These images demonstrate how the annular array can achieve excellent image quality as the range between the transducer and the eye is shifted over a range of 6 mm, whereas a fixed focus achieves high image quality over only a 1- to 2-mm range.

## Discussion

Current very high-frequency ultrasound systems for evaluation of the anterior segment of the eye are constrained by

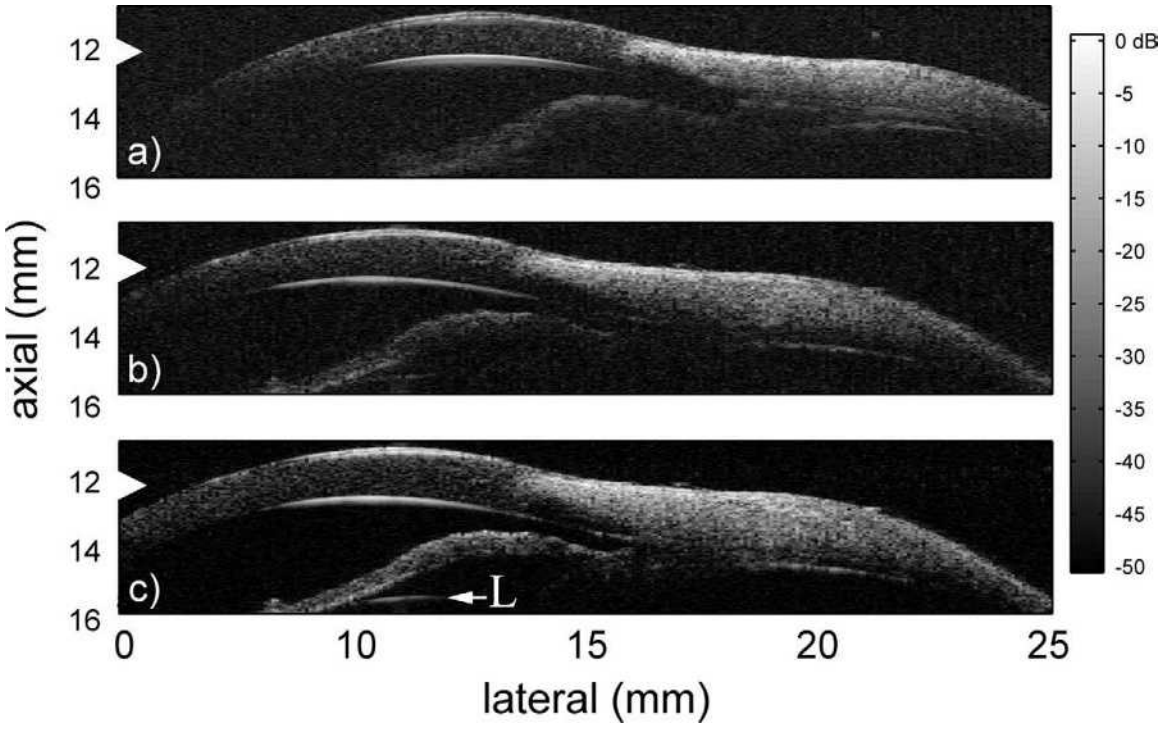


**Figure 6.** Anterior segment images of an ex vivo bovine eye showing data from (**a**) a focused single-element transducer, (**b**) the array with no delay corrections, and (**c**) the array with synthetic focusing (41 focal zones, 120 $\mu$m/zone). Note the improved depiction of the iris and lens surface (L) with synthetic focus. The signal-to-noise ratios were (**a**) 41 decibels (dB), (**b**) 45 dB, and (**c**) 51 dB. White triangles, geometric focus.

their very limited DOF. This results in reduced sensitivity and degraded resolution outside a focal zone that measures less than 1 mm in axial extent. In this report, we demonstrated performance of an annular array transducer operating in the same frequency range as current single-element ultrasound biomicroscopy systems. We showed that this technology can provide a 6-fold increase in DOF.

A limitation of the annular array as currently configured is acquisition speed. In the current system, 5 passes (1 for each ring) are needed to acquire a single image. Further-

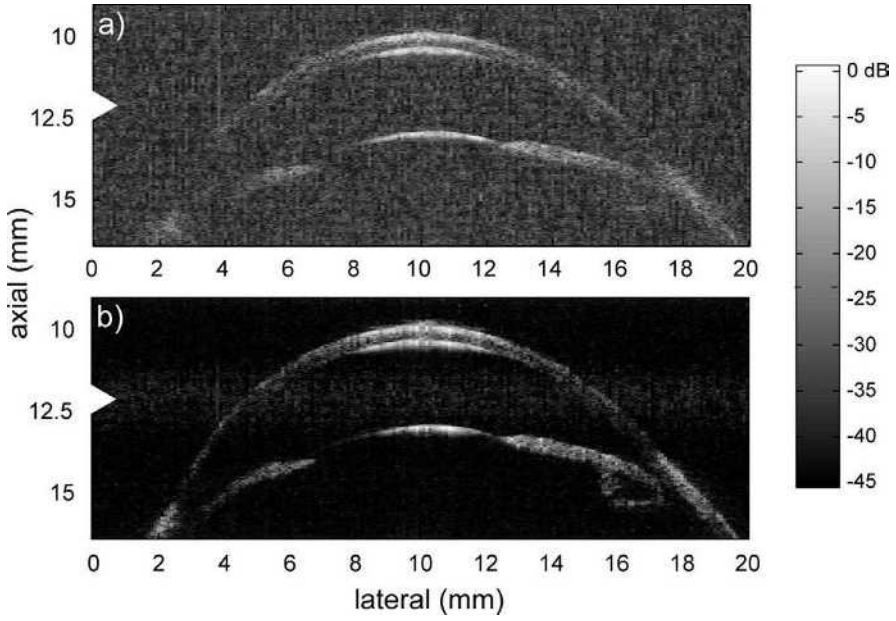


**Figure 7.** In vivo anterior segment scan of a rabbit with (**a**) no delay corrections and (**b**) synthetic focusing (41 focal zones, 177 $\mu$m/zone). The signal-to-noise ratios were (**a**) 35 decibels (dB) and (**b**) 41 dB. White triangles, geometric focus.

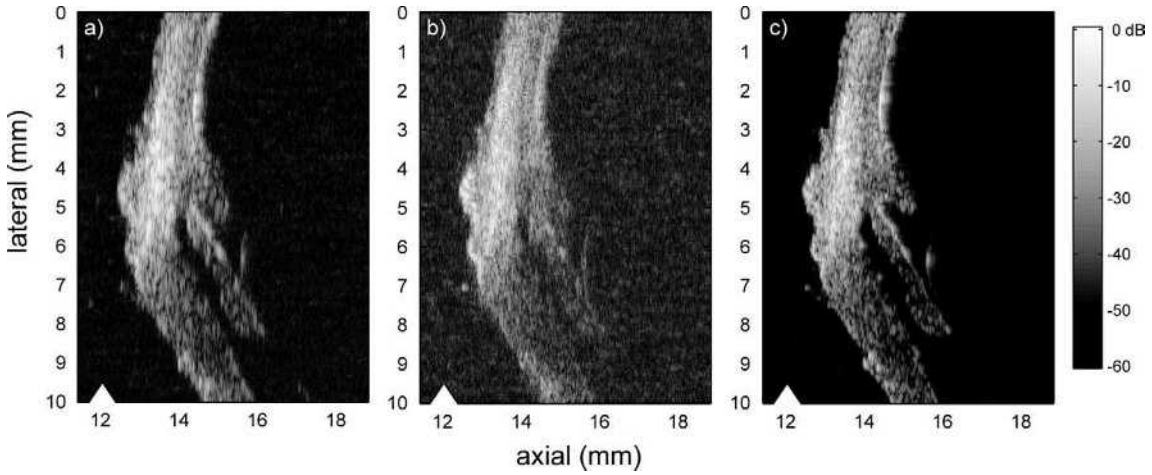


**Figure 8.** Images of the anterior segment of a cadaver eye showing data from the (**a**) center array element, (**b**) full array with no delay corrections, and (**c**) full array with synthetic focusing (41 focal zones, 177 $\mu$m/zone). The signal-to-noise ratios were (**a**) 43 decibels (dB), (**b**) 43 dB, and (**c**) 51 dB. White triangles, position of the geometric focus.

more, data transfer and the processing to form images add additional time constraints. These limitations largely are a result of the prototype nature of the current device. High-speed switching or dedicated pulsers for each element would allow each of the 5 annuli to be excited sequentially at each scan position so that only a single pass would be required to form an image. High-speed data transfer and storage also would reduce overhead. The use of digital signal microprocessors could reduce significantly the time needed to form synthetically focused images as compared with that required when performing these operations in software, as is done in the current configuration. Using presently available technology, speeds of 5 to 10 frames/second are obtainable.

The improved resolution and sensitivity offered by annular array technology will provide significant practical advantages in diagnostic imaging of anterior segment anatomic and pathologic features. Furthermore, this technology can be extended readily to lower frequencies, such as 20 to 25 MHz, that would allow improved assessment of vitreoretinal pathologic features. In summary, we have demonstrated a prototype 40-MHz array transducer for imaging of the anterior segment that achieves improved depth of field, sensitivity, and lateral resolution.

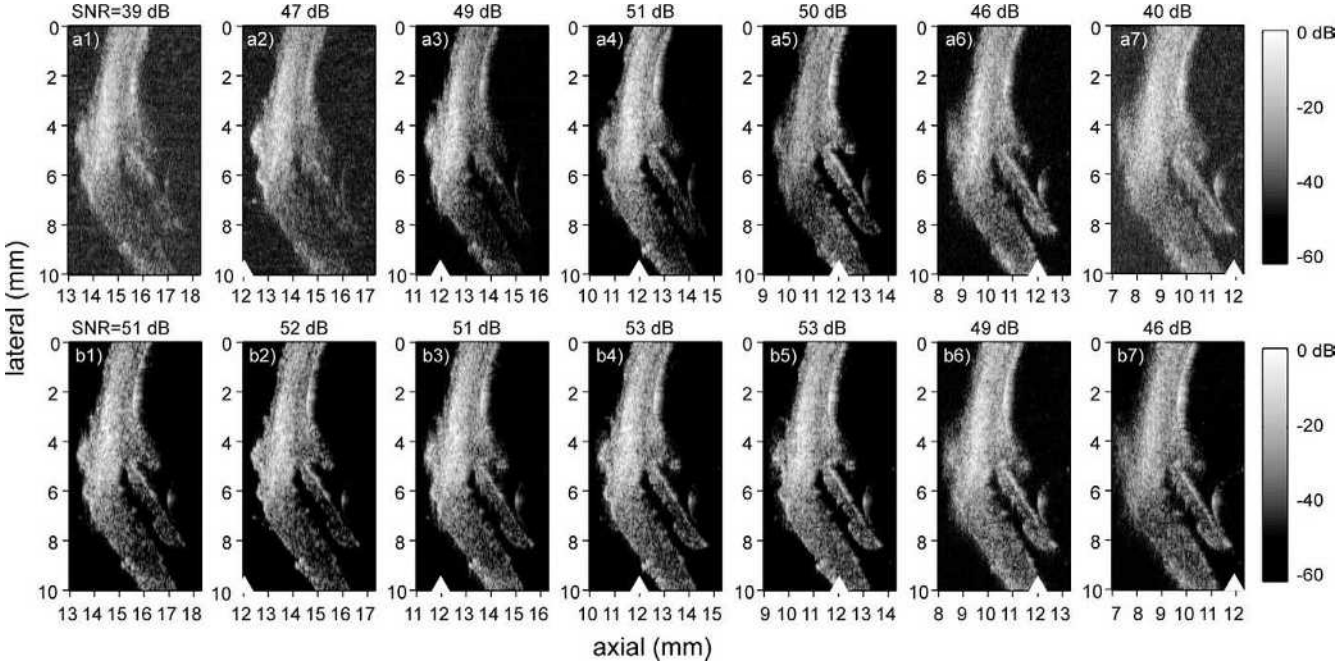


**Figure 9.** Series of anterior segment images of a cadaver eye with the geometric focus (white triangles) progressively incremented by 1-mm axial steps. **a**, Summed data with no synthetic focusing. **b**, Data after synthetic focusing (41 focal zones, 177 mm/zone). Note how image quality is maintained as the range between the transducer and the eye changes when synthetic focusing is used. dB = decibels; SNR = signal-to-noise ratio.

## References


1. Pavlin CJ, Sherar MD, Foster FS. Subsurface ultrasound microscopic imaging of the intact eye. Ophthalmology 1990;97: 244–50.
2. Pavlin CJ, Harasiewicz K, Sherar MD, Foster FS. Clinical use of ultrasound biomicroscopy. Ophthalmology 1991;98:287–95.
3. Pavlin CJ, Harasiewicz K, Foster FS. Ultrasound biomicroscopy of anterior segment structures in normal and glaucomatous eyes. Am J Ophthalmol 1992;113:381–9.
4. Reinstein DZ, Silverman RH, Coleman DJ. High-frequency ultrasound measurement of the thickness of the corneal epithelium. Refract Corn Surg 1993;9:385–7.
5. Reinstein DZ, Silverman RH, Trokel SL, Coleman DJ. Corneal pachymetric topography. Ophthalmology 1994;101:432–8.
6. Reinstein DZ, Silverman RH, Rondeau MJ, Coleman DJ. Epithelial and corneal thickness measurements by high-frequency ultrasound digital signal processing. Ophthalmology 1994;101:140–6.
7. Reinstein DZ, Silverman RH, Raevsky T, et al. Arc-scanning very high-frequency ultrasound for 3D pachymetric mapping of the corneal epithelium and stroma in laser in situ keratomileusis. J Refract Surg 2000;16:414–30.
8. Ritch R, Liebmann JM. Role of ultrasound biomicroscopy in the differentiation of block glaucomas. Curr Opin Ophthalmol 1998;9:39–45.
9. Trope GE, Pavlin CJ, Bau A, et al. Malignant glaucoma: clinical and ultrasound biomicroscopic features. Ophthalmology 1994;101:1030–5.
10. Garcia-Feijoo J, Hernandez-Matamoros JL, Mendez-Hernandez C, et al. Ultrasound biomicroscopy of silicone posterior chamber phakic intraocular lens for myopia. J Cataract Refract Surg 2003;29:1932–9.
11. Kim DY, Reinstein DZ, Silverman RH, et al. Very high-frequency ultrasound analysis of a new phakic posterior chamber intraocular lens in situ. Am J Ophthalmology 1998;125: 725–9.
12. Marigo FA, Finger PT, McCormick SA, et al. Iris and ciliary body melanomas: ultrasound biomicroscopy with histopathologic correlation. Arch Ophthalmol 2000;118:1515–21.
13. Marigo FA, Esaki K, Finger PT, et al. Differential diagnosis of anterior segment cysts by ultrasound biomicroscopy. Ophthalmology 1999;106:2131–5.
14. Deramo VA, Shah GK, Baumal CR, et al. Ultrasound biomicroscopy as a tool for detecting and localizing occult foreign bodies after ocular trauma. Ophthalmology 1999;106:301–5.
15. O'Neil HT. Theory of focusing radiators. J Acoust Soc Am 1949;21:516–26.
16. Cannata JM, Williams JA, Zhou Q, et al. Development of a 35-MHz piezo-composite ultrasound array for medical imaging. IEEE Trans Ultrason Ferroelectr Freq Control 2006;53: 224–36.
17. Hu CH, Xu XC, Cannata JM, et al. Development of a real-time, high-frequency ultrasound digital beamformer for high-frequency linear array transducers. IEEE Trans Ultrason Ferroelectr Freq Control 2006;53:317–23.
18. Brown JA, Demore CE, Lockwood GR. Design and fabrication of annular arrays for high-frequency ultrasound. IEEE Trans Ultrason Ferroelectr Freq Control 2004;51:1010–7.
19. Snook KA, Hu CH, Shrout TR, Shung KK. High-frequency ultrasound annular-array imaging. Part I: Array design and fabrication. IEEE Trans Ultrason Ferroelectr Freq Control 2006;53:300–8.
20. Gottlieb EJ, Cannata JM, Hu CH, Shung KK. Development of a high-frequency (> 50 MHz) copolymer annular-array, ultrasound transducer. IEEE Trans Ultrason Ferroelectr Freq Control 2006;53:1037–45.
21. Ketterling JA, Aristizabal O, Turnbull DH, Lizzi FL. Design and fabrication of a 40-MHz annular array transducer. IEEE Trans Ultrason Ferroelectr Freq Control 2005;52: 672–81.
22. Ketterling JA, Ramachandran S, Aristizabal O. Operational verification of a 40-MHz annular array transducer. IEEE Trans Ultrason Ferroelectr Freq Control 2006;53:623–30.